Optimal Design and Tracking of Descent and Landing Trajectories on Small, Irregular Bodies

Jesús Gil-Fernández, C. Corral van Damme, M. A. Gómez-Tierno

jesusgil@gmv.es

GMV Aerospace & Defence S.A., Isaac Newton 11, Tres Cantos, 28760 Madrid, Spain

Environmental conditions close to small, irregular bodies present many differences compared to major solar-system bodies. In order to achieve precise, soft landing on the surface of a small asteroid, new descent strategies and autonomous navigation systems are required. This paper will focus on the computation of the optimal descent trajectory following a set of waypoints and the autonomous optimal control tracking the reference trajectory. The optimal thrust profile fulfilling the boundary conditions is computed with a direct method. The proper discretization of the dynamics allows obtaining analytical, explicit solution for the dynamics. The constrained parameter optimization problem can be solved analytically although a few iterations are needed to compensate non-linearities. During real operations, environment uncertainties, navigation accuracy and actuators execution errors result in a large landing accuracy. An optimal feed-forward control algorithm is proposed to track the reference descent trajectory. The same discretization than the trajectory design method is used. The control corrections to compensate deviations from the reference trajectory are computed solving analytically different constrained parameter optimization problems. The problem formulation depends on the number of available control variables. The initial guess is the reference thrust profile and no iterations are required for small deviations. When thrust is high enough the control algorithm can be compared with a differential predictive guidance. The latter assumes impulsive manoeuvres that change instantaneously the velocity. Performances of the strategy and the control are assessed in a simulator including an autonomous GNC prototype.

Nomenclature

x_k	=	state vector (position and velocity) at time t_k between two waypoints
u_k	=	control acceleration at time t_k
$\tilde{g}_K$	=	constant gravity acceleration term from linear expansion at time t_k
m_k	=	SC mass at time t_k
J	=	cost function
$\Phi_{N,0}$	=	transition matrix from time t_0 to time t_N
$\Psi_{N,0}$	=	input influence matrix from time t_0 to time t_N
$\{u_k\}_{1,N}$	=	column vector resulting from the concatenation of vectors from index 1 to index N
$\Delta\vec{x}_N$	=	residuals of the final state
$:\prod_{K=0}^{N-1} f_K :$	=	time-ordered product, oldest function placed at the right
T_{max}	=	maximum thrust

I. Introduction

After the success of the Hayabusa mission, there are several missions under study to explore small Near-Earth-Objects (NEO). One of the main scientific benefits of such missions will result from bringing back to Earth a certain amount of asteroid material. These sample-return missions demand a precise, soft landing on specific locations on the asteroid surface in order to take the soil samples. Current studies demand a landing accuracy of few meters, which is an order of magnitude lower than Hayabusa's requirements and requires improved guidance, navigation and control (GNC) strategies.

The dynamics in the proximity of the surface of small (maximum size ~1 km), irregular bodies is characterized by small environmental acceleration and slow velocity. This is beneficial for the descent trajectory design because even small thrusters can provide enough control authority to achieve the required final conditions.

There are additional factors that must be considered in the design of optimal descent and landing (D&L) trajectories. One of the driving factors is that the landing phase will be carried out autonomously, i.e. the entire GNC system will operate without ground intervention. The other driving factor is the uncertainty of certain characteristics of the asteroid close to the surface. In particular, the uncertainty in the dynamics and the appearance of the surface introduce significant challenges in the GNC.

There additional mission and system constraints, such as sample contamination, that must be considered in the trajectory design. Considering all these operational constraints, the trajectory is defined by a set of waypoints that must be reached at certain times. Then, the first objective is the definition of the optimal path that takes the spacecraft (SC) from the current waypoint to the subsequent one in the given time.

The second objective is to design a control method that compensates the deviations in the target waypoint due to errors in models, navigation estimate, and actuators execution. As the GNC system will operate autonomously it is important that the reference trajectory generated by the guidance function is highly compatible with the control system, or in other words that the reference trajectory is 'flyable'. It is important to point out that there is no need of autonomous hazard avoidance since the landing region is a priori known to be safe (there are specific local characterization operations and rehearsals above the landing site to provide data for ground confirmation).

The definition of the mission phase that we are dealing with is seen in Figure 1 for a NEAR-like mission. In a Hayabusa mission the definition is the same but the starting point is not a closed-orbit around the asteroid but a hovering point. The descent starts at a low orbit or a hovering point and ends at the low gate. During the descent the landing region might not be visible, the high gate is the point where the landing area becomes visible. The low gate is located in a certain position with respect to the landing site and marks the start of the autonomous operations until touch down. The definitions are applicable to the rehearsals where there is no touch down but stop a certain range.

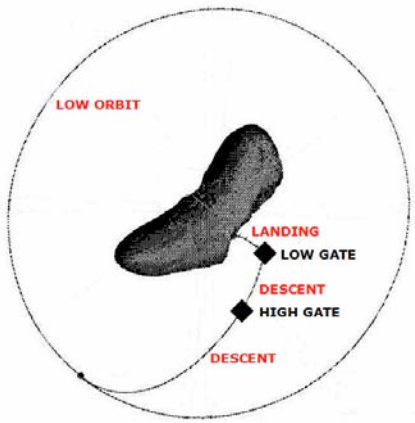

Figure 1. D&L phase definition taking as example the NEAR mission

The first task is to define a set of waypoints and corresponding times that fulfil all the operational constraints and consider the navigation uncertainties and needs. An example of such a set of waypoints starts at 100 m from the desired landing site in radial direction and ends several meters above the landing site in the direction normal to the surface. An example of such trajectory is presented in Figure 2, where the alignment with the normal to the surface is achieved at 15 m altitude.

The waypoints are considered as hold points were the position is maintained for multiple purposes such as sensors acquisition and navigation initialization. In this hold points a state-feedback control reduces the deviation but with low actuator effort, the main purpose is not to achieve the nominal hold point but to prevent drift.

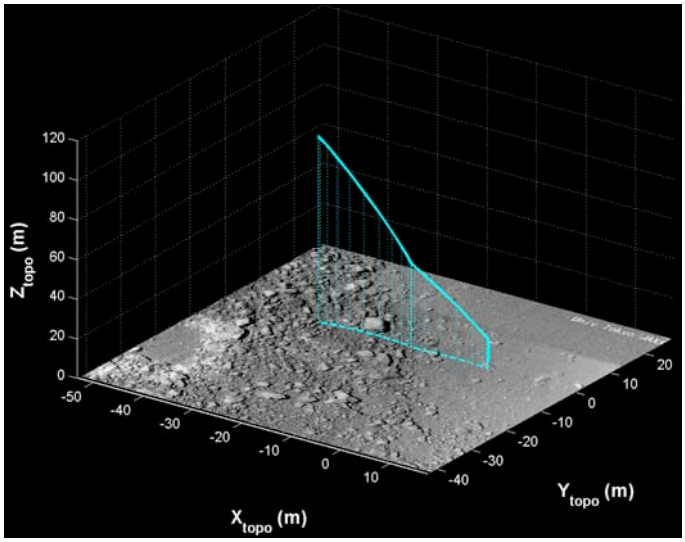

Figure 2. Landing trajectory in topocentric frame

Given the high authority and relatively low propellant consumption in this phase, the thrust structure between waypoints is a 'thrust-coast-thrust'. These '2-burn'-like transfer will achieve any final position and velocity at a fixed time. The final descent before touch-down is executed with a single burn and in open loop to prevent contamination of samples. This final descent is not executed in case of remote sampling (no landing).

There are two scenarios that will be analysed: continuous thrust and impulsive manoeuvres. The impulsive approach is easier to implement on-board. However, when the available thrust makes the impulsive approach not valid because of the inadmissible deviations a more accurate guidance and control approach is required. In addition it must be considered the uncertainties of the problem, and the continuous thrust approach is more robust than the guidance-only impulsive strategy.

II. Descent Trajectory Design

A. Continuous thrust

The problem to solve is a typical fixed-time transfer with specified initial and final conditions. The cost function to minimize is the integral of the square norm of the control acceleration (there are independent thrusters in each direction). We selected a direct optimization method to solve the problem. The discretization of the dynamics follows the model presented by Carson and Acikmese[1]. The time interval between hold points is segmented. In each segment, the gravity field is approximated by a linear expansion and the control acceleration and the zero-order hold approach is used for the control. Finally, the angular velocity of the asteroid is assumed constant (very realistic assumption during the time of the D&L). With this model the dynamics is formulated as a piece-wise Linear Time Invariant (LTI) system.

$$\dot{\vec{x}}_K = A_K \vec{x}_K + B(\tilde{g}_K + \vec{u}_K) \tag{1}$$

The dynamics can be integrated and the state vector at any time can be known through the transition and input-influence matrices (calculated analytically for a given initial position and control).

$$\vec{x}_N = \underbrace{\prod_{K=0}^{N-1} \Phi(A_K; t_{K+1} - t_K)}_{\Phi_{N,0}} \vec{x}_0 + \Psi_{N,0} \left\{ \tilde{g}_K + \vec{u}_K \right\}_{K=0,N-1} \tag{2}$$

With this discretization, the cost function becomes the sum of squares of the control acceleration and the trajectory design problem becomes a constrained parameter optimization problem. This problem is solved by

adjoining the final state constraints to the cost function via Lagrange multipliers. The procedure is formulated and in Ref. 2 and only a summary is provided next with the relevant particularities of the current mission.

The number of segments depends on the control time-step (in the design procedure it is a multiple of this time-step is used) but for the trajectory design the problem is always over-determined. The initial guess is the translation into a finite burn of the impulsive problem, presented in the next section. The Newton steps to reduce the residuals on the final state are computed analytically (3) and the solution is found in few steps.

$$\delta\{\vec{u}_K\} = \Psi_{N,0}{}^T \left(\Psi_{N,0}\Psi_{N,0}{}^T\right)^1 \Delta\vec{x}_N \tag{3}$$

Given the analytical formulation of the optimization problem, with explicit closed-form transition and input-influence matrices, and the fast convergence of the problem, this method is suitable for on-board implementation. The decision of ground-based or on-board guidance implementation depends on the mission considerations such as on-board resources. However, the on-board implementation provides more robustness to large model errors or off-nominal conditions (for instance model errors are likely to happen the first time a descent is carried out over a certain landing site).

B. Impulsive manoeuvres

For high thrust configurations, the design of the trajectory is based on the differential guidance proposed by Battin[3]. The method considers instantaneous velocity changes, therefore equation (2) still holds but there is no control acceleration. The only control variables are the initial impulse ΔV_1 to achieve the final position and the final impulse ΔV_2 to achieve the final velocity (4). Equation (4) defines a determined system and can be solved explicitly. This guidance method is considered for assessment of the previous optimal continuous thrust.

$$\begin{Bmatrix} \vec{r}_N \\ \vec{v}_N \end{Bmatrix} = \Phi_{N,0} \begin{Bmatrix} \vec{r}_0 \\ \vec{v}_0 + \Delta V_1 \end{Bmatrix} + \begin{Bmatrix} 0 \\ \Delta V_2 \end{Bmatrix} \tag{4}$$

III. Trajectory Tracking

A. Continuous thrust

When the reference trajectory is flown there are real world model errors and system execution errors. Therefore, there are deviations from the reference trajectory that must be corrected. For this case we are using a feed-forward control where the model of the plant is given by (1). The design of the control is based on solving a finite-horizon optimal control problem similar to the design problem but in this case the cost function is the corrections to the nominal control acceleration (5).

$$\min_{\delta\{\vec{u}_K\}} J = \sum_{K=0}^{N-1} \left\|\delta\vec{u}_K\right\|^2 \quad \text{, subject to}$$

$$\begin{cases} \dot{\vec{x}}_K = A_K\vec{x}_K + B(\tilde{g}_K + \vec{u}_K), \ \forall k = 0,...,N-1 \\ \vec{x}_N = \vec{x}_F \\ u_{K,i} \in [-a_{K\max}, a_{K\max}], \ \ \forall i = 1,...,3 \ , \forall k = 0,...,N-1, \ \ \text{where } a_{K\max} = -T_{\max}/m_K \end{cases} \tag{5}$$

Then at any time of the descent trajectory the navigation update provides a state that is not in the reference trajectory and the control profile must be updated to achieve the final state. As in the design case, the discrete dynamics can be solved analytically and the final state in (5) is known analytically through a linear system (2). This system is solved in the same way than the optimal trajectory design assuming that a small variation in the nominal control $\delta\{\vec{u}_K\}$ compensates a small deviation in the initial state $\delta\vec{x}_0$.

Each segment provides 3 control variables, therefore when there are less than 3 segments the problem is not over-determined and the optimization makes no sense. In these cases, near the final waypoint, the same procedure to solve the unconstrained problem described in Ref. 2 is implemented. For 2 segments, the problem becomes a simple linear equation solution, and for 1 segment the new cost function is the quadratic norm of the residuals.

$$\delta\{\vec{u}_K\} = -\Psi_{N,0}{}^T\left(\Psi_{N,0}\Psi_{N,0}{}^T\right)^{-1}\Phi_{N-1,0}\delta\vec{x}_0\,,\quad N>2$$
$$\delta\{\vec{u}_K\} = -\Psi_{N,0}{}^{-1}\Phi_{N-1,0}\delta\vec{x}_0\,,\quad N=2 \qquad (6)$$
$$\delta\{\vec{u}_K\} = -\left(\Psi_{N,0}{}^T\Psi_{N,0}\right)^{-1}\Psi_{N,0}{}^T\Phi_{N-1,0}\delta\vec{x}_0\,,\quad N=1$$

The algorithm can be applied to a fixed horizon or a receding horizon problem. In the simulations run so far no iterations are needed, i.e. the system converges with the correction provided at the first iteration. The saturation of the thrusters can be considered in the optimization solution (see Ref. 2 for more details). However, in the current GNC architecture there is common block to include non-linearities such as thrusters saturation or minimum impulse bit (MIB). Therefore, such non-linear effects are common to all the control blocks and is therefore not included for the moment. Should the saturation of the thrusters in the feed-forward control for the continuous thrust becomes frequent, the algorithm would be modified to include boundary projection of the segments with active constraints and repeat the optimization removing these segments[2].

B. Impulsive manoeuvres

The tracking scheme is based in executing trajectory corrective manoeuvres (TCM) at predefined times. Figure 3 depicts an example of the descent trajectory and the location of the main '2-burn' impulses and the TCM. Therefore, the same differential guidance algorithm presented for the trajectory design is applicable in this case.

The main difference is that the initial conditions are only known in real time when the navigation updates the current state. In a case with very high thrust available, the final state can be reached provided that the navigation error converges to zero and there are enough TCM during the descent. However, the effect of the finite thrust in the cases of study always introduces an error in the final position that might be significant.

The manoeuvres are executed in open loop, i.e. the direction is kept constant during the thruster operation and the accumulated delta-V is computed with the thruster model so that the number of control cycles is known.

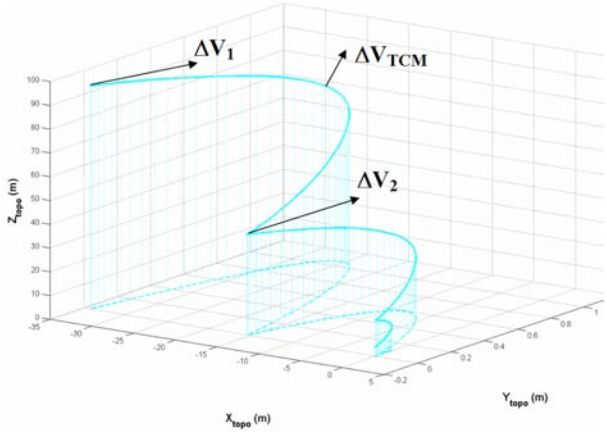

Figure 3. Differential guidance scheme for trajectory design and tracking

IV. Performances Assessment

The benchmark scenario for assessment of the performances of the guidance and control (G&C) algorithms considers a sample return mission to asteroid1999JU3. The most relevant characteristics of the NEO are the rotation period (7.63 h), the mean radius (540 m) and the mass (9.89e11 kg). An example of the type of landing trajectory is presented in Figure 4. The SC mass is 1000 kg.

The G&C strategies are implemented in an autonomous GNC system embedded in a functional engineering simulator. The simulator includes global performances models for the sensors, actuators and attitude control system (ACS). The sensors of the GNC system are a wide angle camera, with the corresponding image processing function, and a set of miniature radar altimeters. The thruster configuration is such that acceleration in any direction can be executed without rotating the vehicle. The environment simulation includes the dynamics affects on the SC and the asteroid topography and surface roughness impact on the measurements.

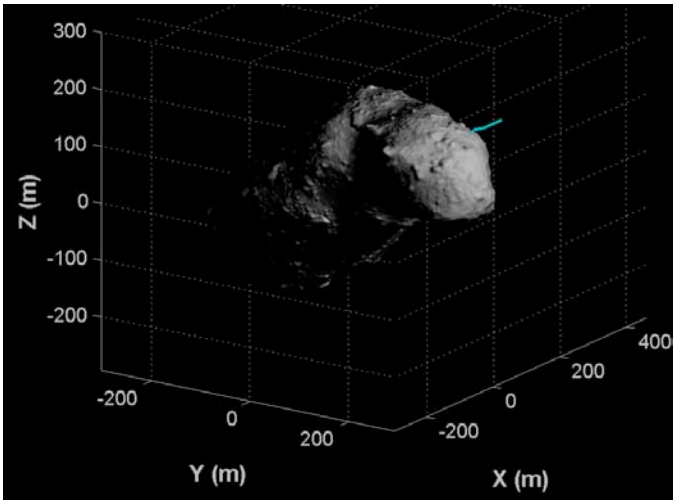

Figure 4. Landing trajectory in the reference scenario (Itokawa shape model used for illustration purposes)

The GNC algorithms include an unscented Kalman filter, which performs a navigation switch at a certain altitude (15 m in the benchmark scenario) from absolute navigation (known landmarks) to relative navigation (unknown landmarks). The guidance function for the impulsive manoeuvres is computed in the on-board SW while for the continuous thrust is preloaded from ground, although as we mentioned this a mission design decision since the algorithm is simple enough to be part of the on-board software and will increase the robustness of the system to large uncertainties or model errors. During the hold points the control function implements a Linear Quadratic Regulator (LQR) to maintain the nominal position.

A. Continuous thrust with 10 N

The reference trajectory and control profile are depicted in Figure 5. The phase starts at 100 m in radial direction (see offset in X coordinates) and finishes at 4 m above the landing site in the direction of the normal to the surface. The landing accuracy and the horizontal velocity at touch down are depicted in Figure 6 for a short Monte Carlo simulation. The summary of the GNC performances for this batch simulation are presented in Table 1. These figures are well below the requirements providing some margin for increase when high-fidelity simulations are executed.

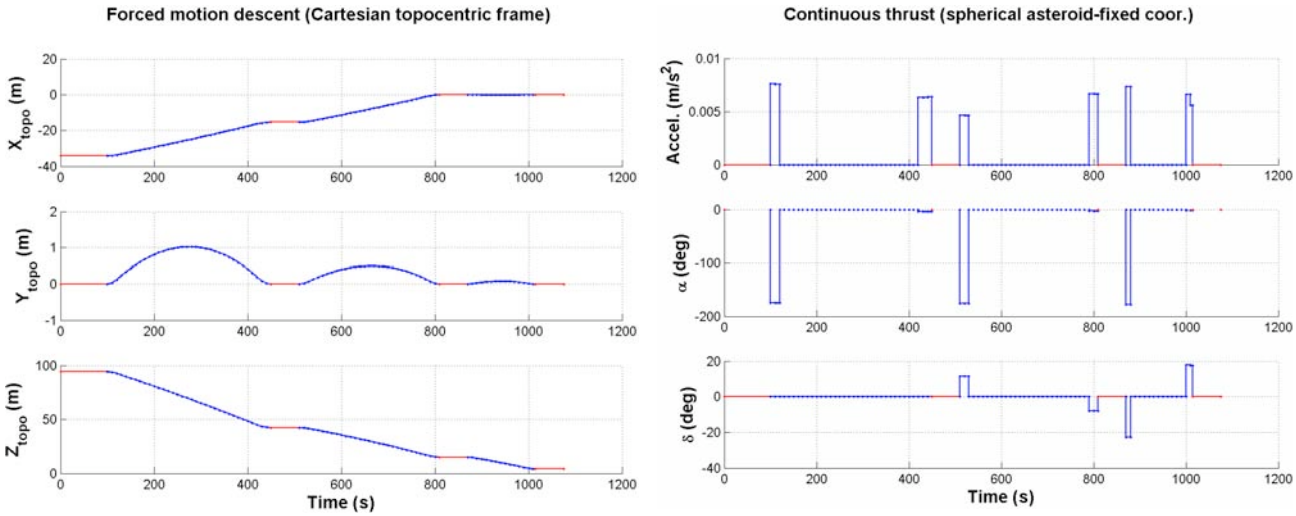

Figure 5. Continuous thrust (10 N) nominal trajectory (coordinates in topocentric frame) and thrust profile (red arcs indicate hold points).

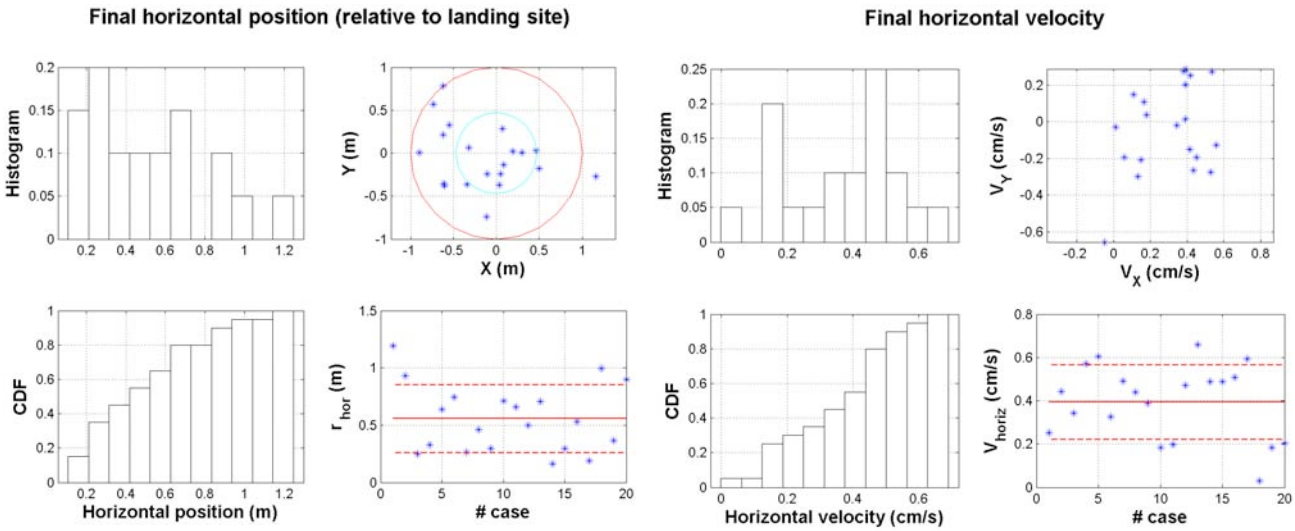

Figure 6. Continuous thrust G&C landing performances (10 N).

Table 1. GNC performances at landing for continuous thrust with 10 N

Performance	Average	Standard deviation	Maximum	Minimum
Delta-V (m/s)	1.19	0.05	1.27	1.09
Horizontal Position (m)	0.56	0.30	1.19	0.16
Horizontal velocity (cm/s)	0.39	0.17	0.66	0.03
Vertical velocity (cm/s)	5.67	0.21	5.99	5.17

B. Impulsive manoeuvres with 10 N

The nominal trajectory is essentially the same than in the continuous thrust case for this level of thrust. The same performances are presented for comparison, landing accuracy and horizontal velocity in Figure 7 and the overall GNC performances in Table 2. Only one TCM at the middle of the interval is included. The landing accuracy is nearly twice that of the continuous thrust confirming the lack of robustness in the presence of model errors (in this case the gravity field has 10% of random error, the solar radiation pressure is one of magnitude lower).

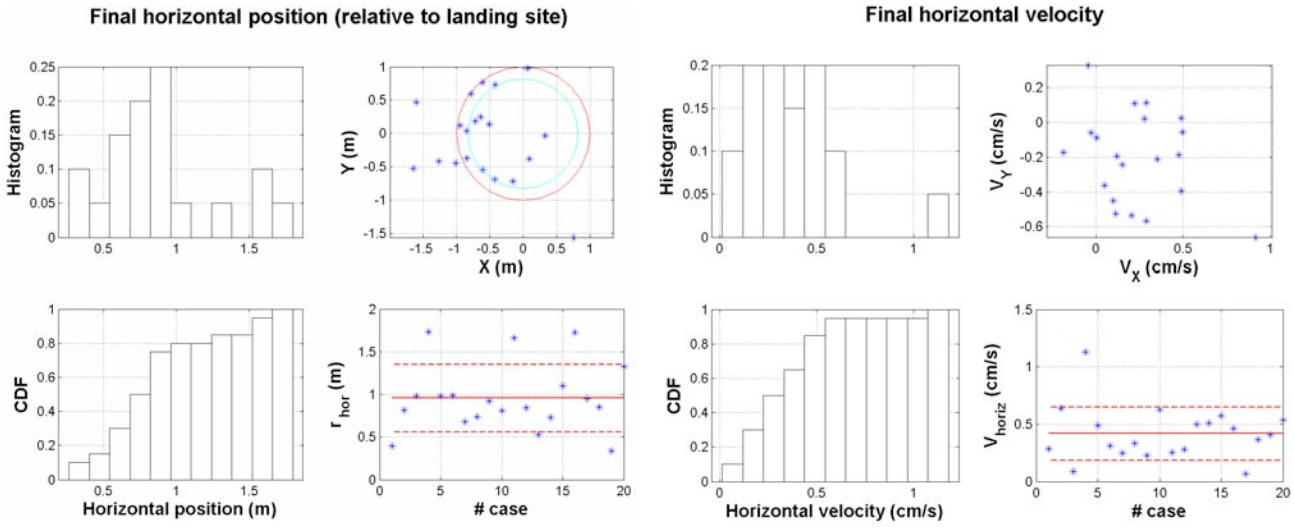

Figure 7. Impulsive manoeuvres G&C landing performances (10 N).

Table 2. GNC performances at landing for impulsive manoeuvres with 10 N

Performance	Average	Standard deviation	Maximum	Minimum
Delta-V (m/s)	1.14	0.10	1.35	0.94
Horizontal Position (m)	0.95	0.36	1.73	0.33
Horizontal velocity (cm/s)	0.42	0.23	1.13	0.07
Vertical velocity (cm/s)	5.62	0.21	5.99	5.17

C. Continuous thrust with 1 N

When the available thrust is 1 N the landing trajectory must be designed accordingly and slower descents are necessary. The coordinates and control acceleration are depicted in Figure 8 (compare with Figure 5). The overall GNC performances from Monte Carlo simulation are summarized in Table 3 and the horizontal position and velocity at landing are presented in Figure 9.

Comparison with results from 10 N (Table 1) shows that the landing conditions are the same. The main source of error is the navigation accuracy being the G&C contribution negligible. The delta-V is lower because the descents are slower, therefore the accelerating and braking manoeuvres are smaller. The case with differential guidance and just 1 TCM gives results much worse and far above the requirements. For this strategy to be applicable a very slow descent with many hold points or TCM would be required and is not acceptable from mission constraints.

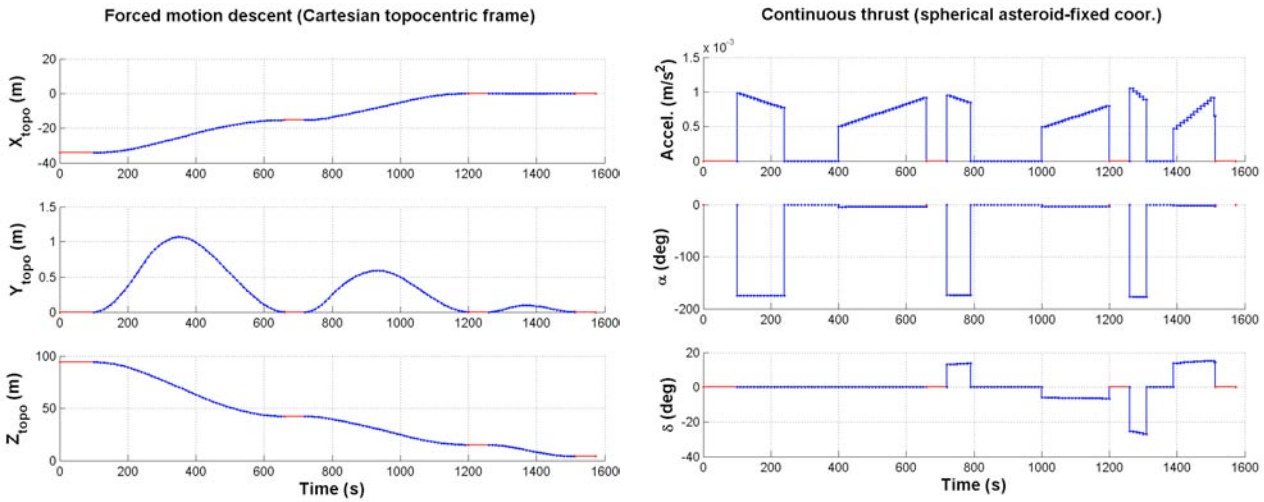

Figure 8. Continuous thrust (1 N) nominal trajectory and thrust profile (red arcs indicate hold points).

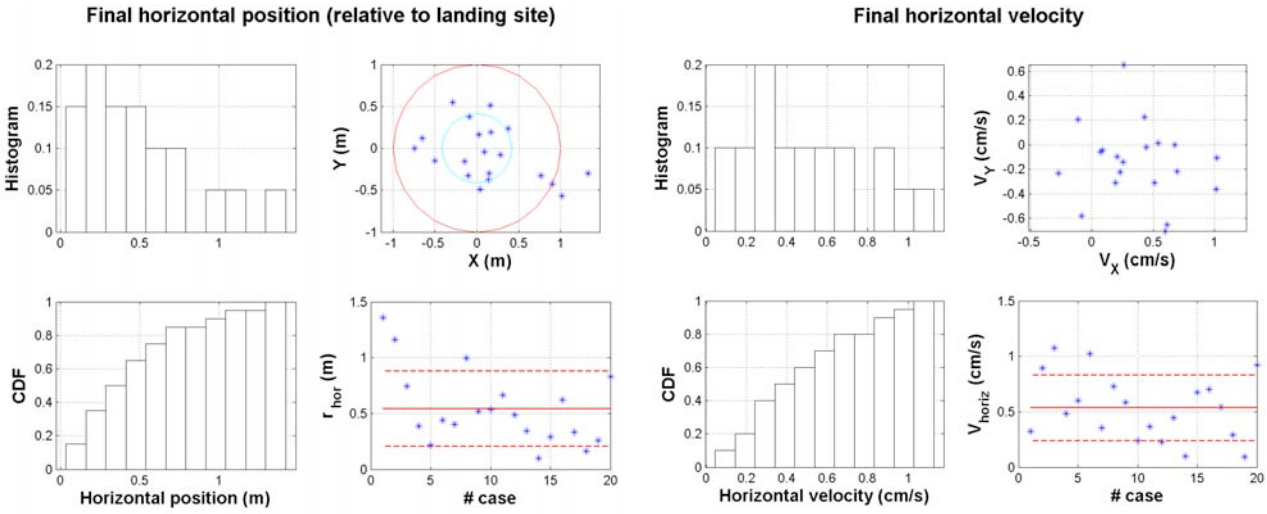

Figure 9. Continuous thrust G&C landing performances (1 N).

Table 3. GNC performances at landing for continuous thrust with 1 N

Performance	Average	Standard deviation	Maximum	Minimum
Delta-V (m/s)	0.91	0.06	1.05	0.81
Horizontal Position (m)	0.54	0.34	1.36	0.10
Horizontal velocity (cm/s)	0.53	0.29	1.08	0.09
Vertical velocity (cm/s)	5.93	0.22	6.38	5.38

V. Conclusions

'Simple' and effective guidance and control algorithms have been developed for autonomous precise landing on small, irregular bodies. The strategy uses continuous thrust approach and the algorithms include explicit, closed-form solutions for the discrete dynamics.

The guidance part solves a fixed-time transfer with a direct method that shows wide radius of convergence due to the great control authority. The optimization solver uses the analytical derivatives from the dynamics and is simple and fast enough to be implemented on-board.

The control function for the descents is a feed-forward optimal control similar in concept to the guidance method. The same analytical derivates from the explicit solution of the dynamics are available and therefore the method is well suited for on-board implementation. In the Monte Carlo simulations for performances assessment no iterations were required for convergence.

In the simulations with the complete GNC prototype the performances of the continuous thrust strategy showed that the main source of error in the landing accuracy was the navigation function, being the G&C contribution at least one order of magnitude lower. These results should be confirmed using high-fidelity simulations.

A classical differential guidance method was implemented for assessment of the continuous thrust approach. Using a 2-burn descent and 1 intermediate TCM the results were much worse than the continuous guidance for 10 N thrust, when the impulsive approach is meaningful, and not even comparable for the 1-N case.

References

[1]Carson, J.M., and Acikmese, A.B., "Small body GN&C research report: A guidance and control technique for small-body proximity operations with guaranteed guidance resolvability and required thruster silent time", JPL Document D-32948, Clearance #05-2804, Jet Propulsion Laboratory, California Institute of Technology, September 2005.

[2]Gil-Fernandez, J., Graziano, M., Milic, E., and Gómez-Tierno, M.A., "Guidance Scheme for Autonomous Electric Propelled Spacecraft", *Space Technology*, ST2430, Lister Science, 2004 (presented in *54th International Astronautical Congress*, Bremen, 2003, IAC-03-A2.08)

[3]Battin, R. H., *Astronautical guidance*, McGraw-Hill, 1964